 https://doi.org/10.3311/PPci.21017

Periodica Polytechnica Civil Engineering, 67(2), pp. 518–529, 2023

Flexural Performance of Composite RC Beams Having an ECC Layer at the Tension Face

Sajjad Wali Khan[1], Yousaf Ali[1], Fasih Ahmed Khan[1*], Muhammad Fahim[1], Akhtar Gul[1], Qazi Sami Ullah[1], Shams-ul-Islam[2]

[1] Department of Civil Engineering, University of Engineering & Technology, Jamrud Road, Peshawar, KPK, Pakistan
[2] Peshawar Development Authority, Hayatabad, Peshawar, Pakistan
[*] Corresponding author, e-mail: fasihahmad@uetpeshawar.edu.pk

Received: 17 August 2022, Accepted: 26 January 2023, Published online: 09 February 2023

Abstract

This paper presents an experimental study on the flexural behavior of composite Reinforced Concrete (RC) beams having a monolithic Engineered Cementitious Composites (ECC) layer at the tension face. Due to the brittle nature of normal concrete, clear cover on the tension side of beam cracks results in spalling and corrosion of reinforcement. The proposed technique overcomes the inherent brittle behavior of normal concrete with the incorporation of ECC on the tension face. This also helps in reducing bond-splitting, cover-spalling, and buckling of reinforcement in RC flexural members. For testing purposes, six full-scale beam specimens (225 mm x 300 mm x 2400 mm) with the same reinforcement were cast and tested. Out of six, two specimens were made of conventional concrete, whereas the remaining four (two each) had an ECC layer of 75 mm and 100 mm thick at the tension face respectively. Each specimen was installed with three strain gauges (one each at the midspan top & bottom surface of concrete and one midspan rebar on the tension face) and one LVDT at midspan. The samples were then subjected to simple monotonic loading under a third-point bending test as per ASTM C78. The load-displacement, stress-strain and moment-curvature curves were obtained for all the tested specimens. It was found that ECC-strengthened beam samples displayed an increased flexural performance at first crack, yield, and ultimate load-carrying capacity as compared to conventional RC specimens. Whereas a better crack arrest with even distribution of cracks and improvement in ductility was observed for the ECC-strengthened composite beams.

Keywords

engineered cementitious composites, reinforced concrete beam, monotonic loading, flexural performance, crack pattern

1 Introduction

Reinforced concrete (RC) has changed the face of construction in the past fifty years, with a substantial increase of RC structures in building stocks worldwide. However, the inadequate performance of concrete in tension has led to the development of fiber-reinforced concrete (FRC) which has consequently limited the use of concrete in selected parts of typical structural members [1]. Several researchers are working on the development of new high-performance materials to improve structural performance through its targeted use [2].

As observed in the previous earthquakes, the inherent brittleness of concrete contributes to common failure modes such as bond-splitting, cover spalling, core-crushing, and steel buckling [3]. Due to cracking and cover spalling, the reinforcement of the structural member is exposed to moisture penetration, causing reinforcement corrosion and consequently leading to section loss of reinforcement and de-bonding of reinforcement, thus jeopardizing the composite behavior of reinforced concrete. The evaluation of various RC members at different ages was carried out by ACI 201.2R-16 [4]. The findings show that many of them were below the structural safety level and need strengthening to improve the load-carrying capacity and durability. When RC structures were subjected to flexural stresses, their deterioration was primarily initiated with exposure of the cover concrete to environmental agents, particularly at the tension face [5]. RC members need a thin cover of relatively ductile and impervious material to prevent bond-splitting failure along the longitudinal bars. Similarly, concrete spalling is very common and

Cite this article as: Khan, S. W., Ali, Y., Khan, F. A., Fahim, M., Gul, A., Ullah, Q. S., Islam, S. "Flexural Performance of Composite RC Beams Having an ECC Layer at the Tension Face", Periodica Polytechnica Civil Engineering, 67(2), pp. 518–529, 2023. https://doi.org/10.3311/PPci.21017

potentially dangerous for RC structures by unnecessarily exposing the reinforcement to moisture. As a consequent corrosion action, the corroded material (rust) occupies ten times more volume, leading to concrete spalling [6].

The use of Engineered Cementitious Composite (ECC), which has improved properties over standard concrete, has shown favourable results in the form of ductility, flexural and tensile strengths [7, 8]. As observed in previous studies, the ECC has a tensile strain capacity of more than 4% [9], with an average tensile strength ranging from 4 MPa to 6 MPa, under which ECC materials are categorized under High-performance fibrer-reinforced cementitious composite (HPFRCC) [10]. This significant tensile strength of ECC is of great importance in improving structural performance in terms of deformation and load-carrying capacities [11]. Strategic use of ECC in conventional reinforced concrete members is found to be very useful [12] in addressing the inherent weaknesses in conventional concrete: from poor ductility and low tensile strength to low energy absorption capacity to lack of self-healing and sulphate-resistant capability [13–17]. The experimental studies carried out by some authors showed that the inherent brittleness of concrete could be overcome through such materials. Unlike conventional concrete, multiple hairline cracks appear in ECC, showing strain-hardening behavior [18]. Such a mechanism of ECC cracking can easily be determined in the matrix by the stress transfer capacity of fibers [19]. This cracks formation behavior of ECC is described as pseudo-ductile behavior with exceptional cracks control with tensile strain up to 3–5% [11].

While keeping the enhanced properties under consideration, a small layer of ECC applied to the tension face of RC beams has proven to be effective in increasing the durability of both concrete and steel reinforcement [20 23]. Under the service load condition, it was found that the ECC layer prevented the migration of aggressive substances into the concrete. Further, experimental studies are reported on the performance of layered composite beams subjected to flexural loads [24–26]. The HPFRCC layer was provided at both the top and bottom faces of the beam, and their study concluded that the layer of HPFRCC at the bottom of the beam section was more effective than using it on the top of the section [24]. Another study reports the flexure behavior of layered ECC-concrete beams and developed a semi-analytical model to predict the flexural performance of composite beams [27].

Although ECC has the potential to change the way buildings are designed and constructed, there is a dearth of both analytical and experimental studies regarding the optimal application of ECC to structural members. Not only is there very little information available on such strategic uses of ECC, but also, they are very uncertain and variable. In light of the literature mentioned above, there is a need to assess the performance of flexure members with varying thicknesses of ECC layers on the tension side. Such beams are tested experimentally to develop an optimum thickness of ECC for RC flexural members.

The current research may be regarded as a step towards adding reliable full-scale experimental data into the pool, which will encourage practising engineers in the field to use ECC confidently for such applications. It will also help in enhancing the structural integrity and durability of structures.

2 Experimental program

2.1 Selection of materials

Ordinary Portland cement (Type-I) and locally available good-quality fine and coarse aggregates were selected for this experimental work. The physical properties of fine and coarse aggregates were evaluated as per ASTM standards, which are presented in Table 1 [28–31]. Fly ash of Type F (see Table 2) and Poly Vinyl Alcohol (PVA) fibers, RECS 15 from Kurarey Company, Japan (as shown

Table 1 Physical properties of fine and coarse aggregates

Characteristics	Fine Aggregate	ASTM Standards	Coarse Aggregate	ASTM Standards
Type	Normal		Crushed	
Specific Gravity	2.51	C 128 [28]	2.56	C 128 [28]
Dry Rodded Bulk Density	2.37 g/cm^3	C 29 [29]	1.63 g/cm^3	C 29 [29]
FM	2.3	C 136 [30]	-	
Absorption %	1	C 128 [28]	1.31	C 127 [31]

Table 2 Chemical composition and physical properties of the fly ash

Parameters	Results %
Silica as SiO_2	60.10
Aluminium as Al_2O_3	24.80
Iron as Fe_2O_3	6.74
Calcium as CaO	7.54
Magnesium as MgO	ND
SO_3	2.61
Loss of Ignition (LOI)	1.03
Specific Gravity	2.1 to 2.2
Colour	Dark Grey
Geometry	Spherical (Glassy)

Fig. 1 Polyvinyl alcohol (PVA) fibers from Kurary Japan, used in ECC

in Fig. 1), were used in ECC. The structural, geometric, and material properties of the PVA fibers used in this study are shown in Table 3. Chemical admixture Chemrite AG–300 (a high range water reducing agent; superplasticizer in brown colour) was used in ECC to achieve the required workability of the mix. Chemrite AG-300 fully complies with ASTM C-1017 [32] standard for concrete admixture. ASTM A615 [33] Grade 40 steel bars of 13 mm (#4) diameter were used as longitudinal reinforcement in RC control, RECC 75, and RECC 100 beams. For shear reinforcement, 10 mm (#3) Grade 60 steel bars were used to make the test samples flexure rather than shear critical. Before casting, steel specimens were tested in the laboratory to find their yield and ultimate strengths, percentage elongation, and bending potential to ensure that the steel used in the research work is within permissible limits of ASTM A615 [33]. The test results for the steel specimens are presented in Table 4.

Table 3 Properties of PVA fibers

S/N	Parameters	Value	SPEC
1	Diameter (dtex)	14.4	15.0 ± 3.0
2	Length (mm)	12.0	12.0 ± 2.5
3	Tensile strength (MPa)	1456	1560 ± 325
4	Elongation (%)	5.7	6.5 ± 1.5
5	Young's Modulus (GPa)	37	

2.2 Mix proportioning

Mix proportioning of the constituent materials of concrete was carried out after preliminary tests on the materials for the targeted 28-day compressive strength of 28 MPa for both standard concrete and ECC. Details of the mix proportion are provided in Table 5. As shown in Fig. 2, the mixing of ECC was done according to the procedure proposed by Lepech and Li [34]. Wet densities of both ECC and control concrete (CC) were determined before casting the specimens, which were 1837 kg/m^3 and 2296 kg/m^3 for ECC and CC, respectively.

2.3 Specimens casting and instrumentation

Six full-scale beams (2400 mm × 225 mm × 300 mm) were cast and cured under laboratory conditions. The dimensional and design details of the beam specimens are shown in Table 6 and graphically presented in Fig. 3 for control

Table 5 Mix proportion of Engineered Cementitious Composites

Mix Design	C*	FA*	S*	CA*	w/c	HRWR	Fibers (%)
Control Mix	1	-	2	3	0.32	0.006	-
ECC Mix	1	1.2	0.8	-	0.32	0.012	2

*C-Cement; FA-Fly ash; S-Fine aggregate; CA- Coarse Aggregate w/c-Water to cement ratio; HRWR-High Range Water Reducer

Fig. 2 Mixing of fibers in ECC

Table 4 Test results of the steel rebars used in beam specimens

S.N	Dia.(mm)	Yield strength (MPa)	Ultimate strength (MPa)	Elongation (%)	Effective Dia. (mm)	Weight (kg/m)	Bend Test
1	13	401.4	537.4	18.8	12.4	0.95	Ok
2	13	405.2	543.5	18.8	12.4	0.95	Ok
3	10	503.8	689.4	15.6	9.7	0.58	Ok
4	10	456.0	609.73	18	9.7	0.58	Ok

Table 6 Geometry and other structural detail of the beam specimens both control concrete and ECC

Sample	No.	Length (mm)	Width (mm)	Height (mm)	ECC Layer thickness (mm) at the bottom face	Longitudinal bars dia (mm)	Transverse reinforcement dia (mm)
Control Beam	2	2400	225	300	-	13	10
ECC-75	2	2400	225	300	75	13	10
ECC-100	2	2400	225	300	100	13	10

concrete (Fig. 3(a)), RECC with 75 mm (RECC75) (Fig. 3(b)) and 100 mm (RECC100) (Fig. 3(c)) layer of ECC, respectively. Five 13 mm diameter (#4) bars were provided as longitudinal reinforcement: three and two at the bottom and top, respectively. The transverse reinforcement of a 10 mm diameter (#3) bar was placed @100 mm center to center throughout the entire length of the beam. The clear cover for both the top and bottom of all specimens was 19 mm). During casting, the ECC layer was poured into the bottom of the formwork and left for two hours to allow it to stiffen sufficiently. Conventional concrete was then poured to fill the formwork to the desired dimensions. The specimens' casting and curing were performed per the ACI standard procedure [35], as shown in Fig. 4 and Fig. 5, respectively.

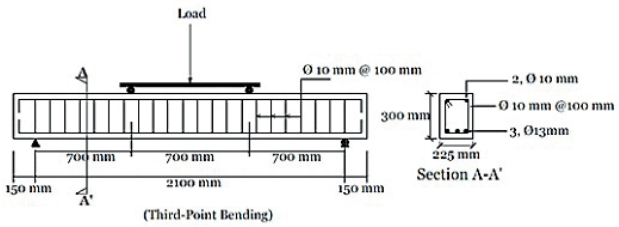

(a)

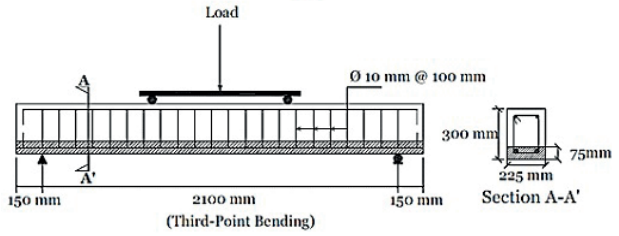

(b)

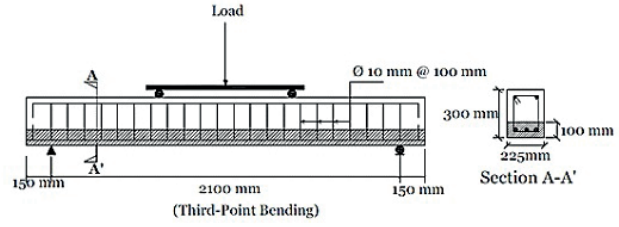

(c)

Fig. 3 Geometry and reinforcement configuration of beams, (a) RC control specimen, (b) RECC 75mm layer specimen, (c) RECC 100 mm specimen

Fig. 4 Casting of full-scale beam specimens

Fig. 5 Curing of full-scale beams, cylinders, and small beam specimens

Representative samples of concrete were also obtained during the casting of beam specimens for the evaluation of compressive, tensile, and flexural strengths after 28 days.

Strain gauges and linear variable differential transducers (LVDTs) were installed at different locations of the beam specimens to measure strain and displacements. During testing, three strain gauges and two LVDTs were installed in each specimen at the midspan. At the bottom surface of the beams, strain gauges with linear dimensions of 60 mm were installed to measure strain at the midspan bottom surface of the beam. Similarly, another strain gauge with a linear dimension of 100 mm was placed at the midspan top surface of the beam to measure the strain at the extreme top fibers. Usually, the surface strain gauges are either deboned or broken during bending; therefore, strain gauges of 6 mm length were also glued at the midspan of the bottom longitudinal reinforcement rebar. Furthermore, two LVDTs were also installed at the midspan of the beam specimens.

2.4 Testing

The tests were divided into two parts; the first one comprised the preliminary tests on the constituent materials for the mix design, including gradation of aggregate, absorption, and chemical composition. After mix design, the mechanical properties (compressive, tensile, and flexural strengths) of both control concrete and ECC were determined as per ASTM standards (Fig. 6 and Fig. 7).

Similarly, to evaluate the workability of fresh concrete, a slump test was performed as per ASTM standard C-143 for a slump value of 50 mm (Fig. 7(a)) as per mix design criteria [36]. Slump values for ECC were calculated by the Hyun-Joon Kong method [37], as shown in Fig. 7(b). According to this method, ECC was poured into the slump cone without any compaction, and the cone was then lifted, allowing ECC to spread on the floor as shown in Fig. 7(b). The slump for ECC was then calculated using Eq. (1).

$$\Gamma = \left(D_1 - D_0\right) / D_0 \geq 2.75\,, \tag{1}$$

where Γ = deformability factor, D_1 = Average of two orthogonal diameters, and D_0 = Diameter of the bottom of slump cone.

The value of the Deformability factor (Γ) was found to be 68 mm (2.76 inches), which is within permissible limits (see Fig. 8) [38].

In the second testing phase, simply supported full-scale beam specimens were tested in a straining frame under the third point bending, as shown in Fig. 8 and schematically represented in Fig. 3. The load was applied continuously at

Fig. 6 Visuals of the tests for determination of the mechanical properties: (a) Compressive (b) Split tensile and (c) Flexural strengths of both control concrete and ECC

Fig. 7 Workability tests of (a) Normal Concrete and (b) ECC concrete

Fig. 8 Testing of the full-scale beam in straining frame under third point bending [38]

a displacement rate of 0.0254 mm/sec till failure. Loads, deflections, and strains were measured through the data acquisition system of a multi-channel data logger (UKM70).

3 Results and discussion

A few parameters of interest were accrued from test data and are presented in the form of tables and figures. The results from the testing of experimental models have been further classified into the following domains.

3.1 Mechanical properties

The average results of specimens tested in a universal testing machine (UTM) for compressive, tensile, and flexural strengths are shown in Fig. 9. The experimental results indicate the superior mechanical properties of ECC over standard concrete. ECC's tensile and flexural strengths are more than twice that of standard concrete, making it an ideal material for use in the tensile regions of RC members.

3.2 Load deflection curves

3.2.1 Control concrete beam

To set a benchmark for comparison purposes, two beam specimens of control concrete were initially tested in the straining frame of 1000 kN capacity. Monotonic loading was applied to the samples from an unstressed state to failure, defined by significant damage to the sample. It can be seen in Fig. 10 that there is a linear relationship between load and deflection till the yield point. At a loading rate of 0.017 mm/sec, the first crack appeared at 55.19 kN and 56.12 kN in RC control beams 1 and 2, respectively, with a corresponding deformation of 4.84 mm and 4.68 mm. Similarly, deformations of 10.10 and 8.50 mm were recorded at yield loads of 107.21 kN and 96.20 kN for beams 1 and 2, respectively. Both the specimens (beam 1 and 2) failed at ultimate loads of 121.52 and 116.71 kN with corresponding deformations of 20.76 and 30.07 mm respectively. The summary of the combined test results for RC control and RC-ECC beam specimens is presented in Tables 7–9 and graphically in Fig. 10.

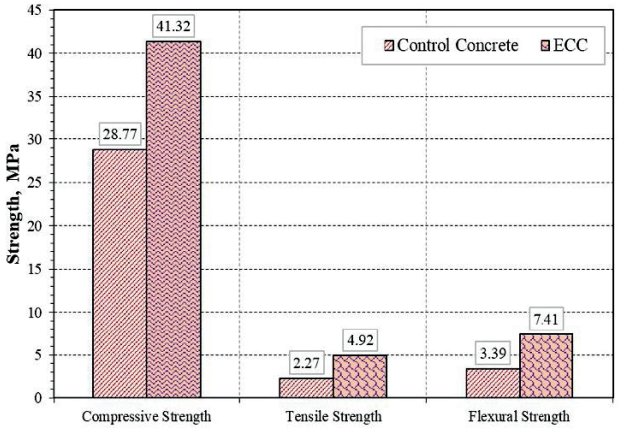

Fig. 9 Experimental results of the compressive, tensile, and flexural strengths of control concrete and ECC

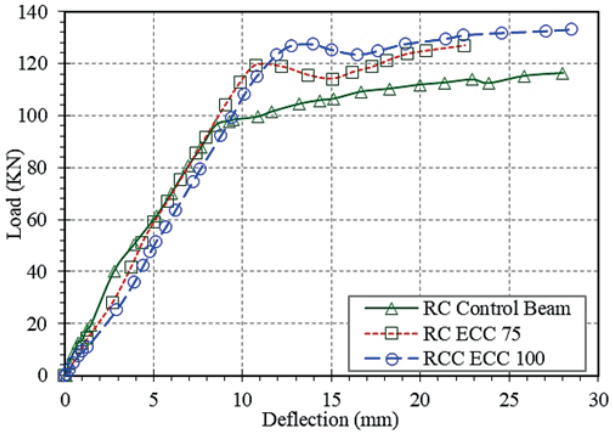

Fig. 10 Combined load-deflection curves

3.2.2 RC-ECC 75 beam

The overall response of RC-ECC 75 beams was the same as control specimens; however, the first crack, yield, and ultimate loads, as well as their corresponding deflections, increased compared to RC-control beams. The first crack in RECC 75 beams 1 and 2 initiated at loads of 74.06 kN and 72.65 kN, respectively, with corresponding deflection values of 6.42 and 8.08 mm. The average Increase in the first crack load and deformation was about 32% and 49.8%, respectively, compared to control specimens. Similarly, the steel yielding for both the specimens took place at loads of 118.35 and 108.04 kN with corresponding displacements of

Table 7 Comparison of cracking, yield, and ultimate load-deflection

S.No	Beam type	P_{cr} (kN)	Δ_{cr} (mm)	P_y (kN)	Δ_y (mm)	P_u (kN)	Δ_u (mm)
1	RC Control Beam 1	55.19	4.84	107.21	10.10	121.52	20.76
	RC Control Beam 1	56.12	4.68	96.20	8.50	116.71	30.07
2	RC ECC 75 Beam 2	74.06	6.42	118.35	10.46	128.07	22.32
	RC ECC 75 Beam 2	72.65	8.08	108.04	12.00	114.25	23.75
3	RC ECC100 Beam 1	94.32	8.92	125.73	12.24	135.65	28.48
	RC ECC100 Beam 2	94.56	9.20	115.89	12.29	120.57	22.02

P_{cr} - Cracking load; P_y - Yield load; P_u - Ultimate load

Table 8 Percentage increase in cracking, yield, and ultimate load-carrying capacities

Beam Description	P_{cr} (kN)	Average Increase (%)	P_y (kN)	Average Increase (%)	P_u (kN)	Average Increase (%)
RC Control Beam 1	55.19	-	107.21	-	121.57	-
RC Control Beam 1	56.12		96.20		116.71	
RC ECC 75 Beam 1	74.06	31.8	118.35	11.3	127.61	1.5
RC ECC 75 Beam 2	72.65		108.04		114.25	
RC ECC100 Beam 1	94.32	69.7	125.73	18.8	135.65	7.52
RC ECC100 Beam 2	94.56		115.89		120.57	

P_{cr} - Cracking load; P_y - Yield load; P_u - Ultimate load

Table 9 Percentage increase/decrease in cracking, yield and ultimate deflection

Beam Description	Δ_{cr} (mm)	Average Increase (%)	Δ_y (mm)	Average Increase (%)	Δ_u (mm)	Average Increase (%)
RC Control Beam 1	4.84	-	10.10	-	20.76	-
RC Control Beam 1	4.68		8.50		30.07	
RC ECC 75 Beam 2	6.42	52.3	10.46	20.75	22.32	-9.0
RC ECC 75 Beam 2	8.08		12.00		23.75	
RC ECC100 Beam 1	8.92	90.33	12.24	31.88	28.48	-1.50
RC ECC100 Beam 2	9.20		12.29		22.02	

Δ_{cr} - deflection at the appearance of first crack; Δ_y- deflection at yield; Δ_u- deflection at ultimate load

Table 10 Comparison of cracking, yield and ultimate moment-curvature values

Beam type	M_{cr}	φ_{cr}	M_y	φ_y	M_u	φ_u	Curvature Ductility Ratio
	(kN-m)	(1/m)	(kN-m)	(1/m)	(kN-m)	(1/m)	φ_u/φ_y
RC Control Beam	19.32	0.0149	37.52	0.0397	39.99	0.1177	2.96
RC- ECC 75 Beam	26.92	0.0189	42.42	0.0646	45.82	0.4108	6.35
RC ECC-100 Beam	34.01	0.0224	45	0.0317	46.73	0.041	1.23

M_{cr} - Cracking moment; M_y - yield moment; M_u - ultimate moment

10.46 mm and 12 mm, respectively. Compared to control concrete specimens, this again shows an average enhancement of 11.3% and 20.75% in the load and deflection, respectively. This trend continued till failure; however, a slight scatter was observed in the deflections at the ultimate point. The average deflections of RC-ECC 75 slightly decreased compared to control specimens (see Table 10). However, ultimate loads for the same increased slightly (1.5%) in comparison to control specimens.

3.2.3 RC-ECC 100 beam

Fig. 11 shows the combined load-deflection curve for RC-control and RC-ECC beam specimens. In RC-ECC 100 beams, the load and deflection pattern were similar to RC-ECC 75 beams, but the performance further improved compared to RC-ECC 75 beams. Details of the experimental results for all the specimens are presented in Table 9 and Table 10. As discussed earlier, the difference (in terms of loads and deflections) is more prominent at first crack and yield points and narrows down while moving towards the ultimate point. There are significant improvements in the cracked (69.7%), yield (18.8%), and ultimate (7.52%) loads as compared to the control. Similarly, the corresponding average Increase in deflections at first crack, yield, and ultimate points were 90.33%, 31.88%, and 0%, respectively. Although a balanced failure was observed in the RC-ECC 100 beam specimen, the beam's stiffness was not significantly reduced before failure and was thus believed to be elastic range.

3.3 Moment curvature

Bending moments were calculated based on combined (applied load plus self-weight) load from the data of the strain gauges mounted at the midspan top and bottom surfaces and bottom longitudinal reinforcement bars. A flexural mode of failure was observed in all beams. The cracking moment of the beams with ECC layers was found to be significantly greater than control specimens (Fig. 12). For example, compared to RC control concrete, the cracking moments of RC-ECC-75 and RC-ECC-100 increased by 39.33% and 76%, respectively. Similarly, the yielding of RC control, RC-ECC 75, and RC-ECC 100 beam

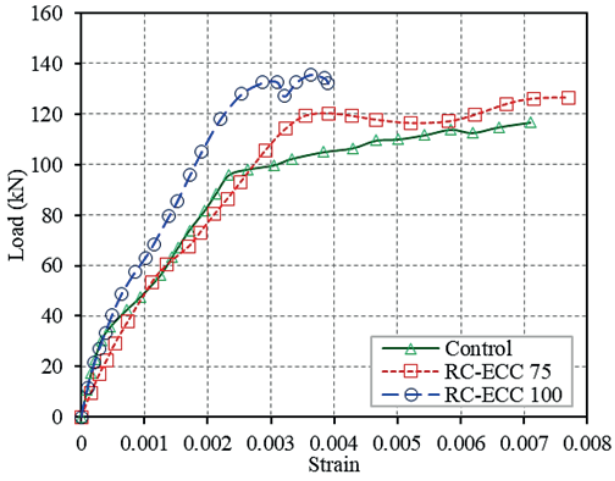

Fig. 11 Combined load versus strain curves

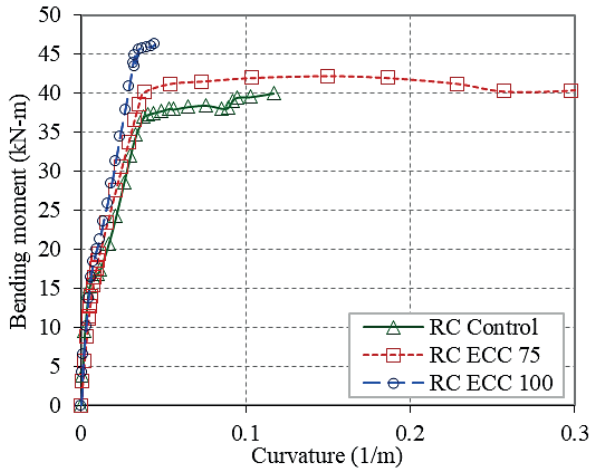

Fig. 12 Combined moment-curvature curves

specimens were found to occur at a moment value of 37.52, 42.73, and 45 kN-m with the corresponding curvatures of 0.0397, 0.0646, and 0.072 (1/m), respectively. Beam specimens with ECC layers exhibited more Curvature and ductility than control specimens. The Increase at the moment after yielding to the ultimate point is slightly zig-zag, spreading over a range of curvatures. The ultimate moments for RC control, ECC 75, and ECC 100 were 39.99, 45.82, and 46.73 kN-m, respectively, with the corresponding curvature values of 0.1177, 0.31, and 0.390 (1/m). The curvature ductility ratios of RC-ECC beam specimens are higher than RC control specimens (Table 10). This ratio has almost doubled for the beam specimen with 100 mm ECC layer at the bottom face.

3.4 Ductility

Ductility is the property under which the structure endures inelastic deformation under applied load before specimen failure without substantial loss in capacity. As shown in Table 10, the ductility was calculated by recording the deflection value at the ultimate point and yield point from the experimental results. The ductility ratio manifests that using the ECC layer in the tension zone of the beam may or may not increase the overall ductility of the beam as it was increased for RC-ECC 75 and decreased for RC-ECC 100. An approximate increase of 136% was observed in ductility for RC-ECC-75, whereas a net percent decrease of 59.4% was noticed for RC-ECC-100 layers compared to control samples. The decrease may be because of compression failure in RC-ECC-100 beams. As the addition of ECC layer in beam strengthened it on tension side and thus demand on the compression side is increased that may be either fulfilled by providing reinforcement or using high-strength concrete.

3.5 Load versus strain

Strain gauges were installed at the midspan of the longitudinal rebar of the beams to measure strain in the rebar. Fig. 11 shows the strain variations with an increase in load till the failure of the beam specimens. The plot shows that the strain increases linearly with the increase in load till the appearance of the first crack in the beam specimens. After the appearance of the first crack, the slope of the lines slightly changed; however, the relationship was still linear till the yielding of the steel. After yielding, strain hardening occurs, and the specimens were still able to take load. ECC layer in the beam delayed initiation of the first crack in the beam and hence the elastic limit of the beam specimens increased, as shown in Fig. 11. The details of the corresponding strains at the first crack, yielding, and ultimate load are presented in Table 11. An increase of 56% and 69% was observed in the yield strain for RC-ECC-75 and RC-ECC-100 beams compared to the control beam. Contrary to this, a decrease of 2.24% and 16.6% in the ultimate strain was observed for both specimens.

3.6 Crack pattern and development

Crack patterns were closely observed for both control and composite beam specimens. Initially the small hairline cracks appeared in the flexure region (between two load-point) of the beam. With further increase in the load, the existing flexural cracks aggravated, leading to the failure of the beams. Its worth mentioning that after the failure of the beam, all the cracks were formed in the mid-region, representing flexural control sections. A detailed discussion of the crack pattern of all the specimens is presented in the following sections.

Table 11 Load versus strain with percent increase/decrease

Beam	P_{cr} (kN)	Strain	Rise (%)	P_u (kN)	Strain	Fall (%)
RC Control Beam 1	55.2	0.00101	-	121.5	0.004	-
RC Control Beam 2	56.1	0.00100		116.7	0.007	
RC-ECC 75 Beam 1	74.1	0.00191	56	127.6	0.0072	-5.5
RC ECC 75 Beam 2	72.7	0.00156		114.2	0.0032	
RC-ECC 100 Beam 1	94.4	0.00169	69	130.6	0.0035	-16.7
RE ECC 100 Beam 2	94.0	0.00206		114.0	0.0052	

P_{cr} - Cracking load; P_u - ultimate load

3.6.1 RC control concrete beam crack pattern

In the RC control beam, the cracks and their pattern were closely monitored and recorded while applying the incremental load on the specimens. Cracks in concrete control specimens were found to initiate at lower load levels than composite beams with an ECC layer at the bottom face. The first crack RC control beam 1 and 2 appeared at a load of 55.19 and 56.12 kN, respectively. Under increasing load, more cracks in the flexure region (midspan) were found to occur and propagated in the vertical direction (see Fig. 13). With a further increase in the load, the vertical cracks in the beam became wider and deeper by propagating toward the compression region. Relatively unstable and fast growth of cracks was observed RC control specimens. At the failure stage, more than ten major (wide) cracks were formed in the beam's middle (see Fig. 13). Crushing of concrete in the RC control beam was found to occur long after the yielding of flexural reinforcement, whereas no shear cracks were observed in the beam.

3.6.2 RC-ECC 75 beam crack pattern

The number of cracks and their distribution and size greatly varied in RC-ECC specimens. The crack distribution for the RC-ECC beam specimen is presented in Fig. 14. The first crack in RC-ECC 75 originated in the composite beam's concrete portion (rather than ECC) at 74.06 and 72.65 kN, respectively. An average improvement of 32% in load-carrying capacity was noted compared to control concrete. Whereas a crack in the ECC layer was observed at an average load of 100 kN, followed by the second and third crack (minor type) at 110 kN and 115 kN, respectively. Furthermore, compared to RC control concrete, the growths of vertical cracks were stable in RC-ECC beam specimens, which shows the effectiveness of the ECC layer in controlling the formation and width of the cracks. Before crushing concrete on the compression face, the ultimate bending moment reached 45.82 kN.m, which is 14.5% higher than the control specimen. Six minor (very small compared to RC control beam) cracks were recorded, out of which a single crack widened up to the compression region leading to the failure of the specimen. It is also worth mentioning that no crack or de-bonding mechanism was observed at the interface of ECC and concrete in any composite specimens.

3.6.3 RC-ECC 100 beam crack pattern

The crack pattern in RC-ECC 100 beam was like RC-ECC 75; however, further improvements were observed in the cracking, yielding, and ultimate bending moments. The first crack in RC-ECC 100 beams 1 and 2 appeared at 94.44 and 94 kN, respectively, in the composite section's concrete portion, as observed in the RC-ECC 75 beam. An average improvement of 70% in load carrying capacity was noted compared to control concrete. Similarly, the first crack in the ECC layer was noted at an average load of 109 kN, followed by another crack at 126 kN. Although few hairline

Fig. 13 Cracks formation and their distribution in RC- control beam

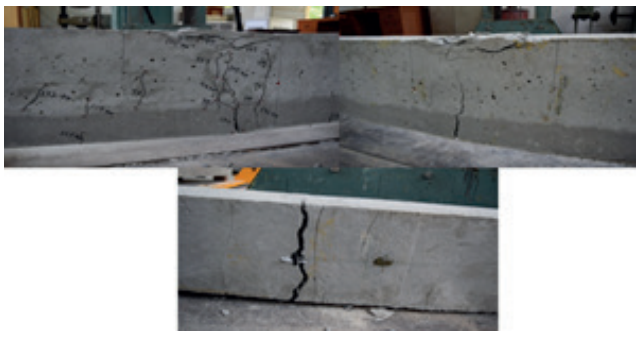

Fig. 14 Cracks formation and their distribution in RECC 75 beam

cracks appeared in the beam, the one at the midspan aggravated and caused the beam specimen failure. At the ultimate stage, the crushing was limited to the upper mid portion of the concrete, as shown in Fig. 15. Just like RC-ECC 75, no crack or de-bonding was observed at the interface of ECC and standard concrete in this case well. The crushing of concrete in this beam is believed to occur before the yielding of flexural reinforcement. No shear cracks in the beam were observed till failure.

Fig. 15 Cracks formation and their distribution in RECC 75 beam

4 Conclusions

After careful analyses of the test results, various conclusions have been drawn. The key conclusions are as follows:

1. The flexural performance of the RC beams was enhanced significantly with the addition of the ECC layer on the tension face in terms of cracking, yield, and ultimate (loads and) moments. As compared to control RC beams, an average increase of 32% and 70% was observed in the first-crack load for layer thicknesses of 75 mm and 100 mm, respectively. The yield load increased by 11% and 19% and ultimately by 1.5% and 7.52% for RC-ECC-75 and RC-ECC-100, respectively. An increase of 39.33% and 76% in the cracking moments were observed for RC ECC 75 and RC-ECC-100, respectively. The yield moments for the two beams increased by 13% and 19% and ultimately by 14.5% and 16.85%, respectively.
2. The incorporation of the ECC layer in the tension zone improved the serviceability by decreasing the number of open wide cracks in the beam specimens to a single crack in the flexure region at the failure stage. Further, the crack growth in ECC composite beams was found to be more stable than in the control specimens. The cracks were found to first appear in the concrete portion rather than the ECC layer. No cracks in the ECC layer may prove very useful in controlling the corrosion of reinforcement and spalling concrete in flexural members.
3. Increasing the thickness of ECC layer was found to increase the overall flexural performance of the beam specimens. However, this may result in a brittle failure on the compression side. To fully exploit its capacity, the beam needs to be strengthened in compression by providing additional reinforcement.
4. No weak zone at the interface of ECC and conventional concrete was observed till the failure of the specimens, which means that a good bond is maintained between ECC and conventional concrete and thus such composite beams can be confidently used in the field.

Acknowledgements

The authors are grateful to the Department of Civil Engineering, University of Engineering & Technology Peshawar, for providing laboratory facilities.

References

[1] Pakravan, H. R., Ozbakkaloglu, T. "Synthetic fibers for cementitious composites: A critical and in-depth review of recent advances", Construction and Building Materials, 207, pp. 491–518, 2019. https://doi.org/10.1016/j.conbuildmat.2019.02.078

[2] Khan, F. A., Khan, S. W., Said, I., Hussain, S. "An Economical Engineered Cementitious Composite (ECC) prepared with fine quarry sand and a nominal amount of PVA fibers", Cement, Wapno, Beton, 26(4), pp. 323–339, 2021. https://doi.org/10.32047/CWB.2021.26.4.5

[3] Korkmaz, S. Z. "Observations on the Van Earthquake and Structural Failures", Journal of Performance of Constructed Facilities, 29(1), 04014033, 2015. https://doi.org/10.1061/(ASCE)CF.1943-5509.0000456

[4] ACI Committee 201 "ACI - 201.2R-16 Guide to Durable Concrete", ACI Journal Proceedings, 74(12), pp. 573–609, 2016. [online] Available at: http://www.concrete.org/Publications/ACIMaterialsJournal/ACIJournalSearch.aspx?m=details&ID=11047

[5] Maalej, M., Ahmed, S. F. U., Paramasivam, P. "Corrosion Durability and Structural Response of Functionally-Graded Concrete Beams", Journal of Advanced Concrete Technology, 1(3), pp. 307–316, 2003. https://doi.org/10.3151/jact.1.307

[6] Val, D. V., Chernin, L., Stewart, M. G. "Experimental and Numerical Investigation of Corrosion-Induced Cover Cracking in Reinforced Concrete Structures", Journal of Structural Engineering, 135(4), pp. 376–385, 2009. https://doi.org/10.1061/(ASCE)0733-9445(2009)135:4(376)

[7] Li, V. C., Wang, S. "Flexural behaviors of glass fiber-reinforced polymer (GFRP) reinforced engineered cementitious composite beams", ACI Materials Journal, 99(1), pp. 11–21, 2002. https://doi.org/10.14359/11311

[8] Li, V. C., Wang, S., Wu, C. "Tensile strain-hardening behavior or polyvinyl alcohol engineered cementitious composite (PVA-ECC)", ACI Materials Journal, 98(6), pp. 483–492, 2001. https://doi.org/10.14359/10851

[9] Li, V. C. "Integrated structures and materials design", Materials and Structures, 40, pp. 387–396, 2007. https://doi.org/10.1617/s11527-006-9146-4

[10] Ma, H., Qian, S., Zhang, Z., Lin, Z., Li, V. C. "Tailoring Engineered Cementitious Composites with local ingredients", Construction and Building Materials, 101, pp. 584–595, 2015. https://doi.org/10.1016/j.conbuildmat.2015.10.146

[11] Fischer, G., Li, V. C. "Effect of fiber reinforcement on the response of structural members", Engineering Fracture Mechanics, 74(1–2), pp. 258–272, 2007. https://doi.org/10.1016/j.engfracmech.2006.01.027

[12] Khan, F. A., Khan, S. W., Rashid, M., Rizwan, M., Fahim, M., Shahzada, K., …, Said, I. "Evaluation of code compliant/non-compliant ECC-RC IMRF structures", Structures, 32, pp. 1634–1645, 2021. https://doi.org/10.1016/j.istruc.2021.03.070

[13] Song, P. S., Wu, J. C., Hwang, S., Sheu, B. C. "Statistical analysis of impact strength and strength reliability of steel–polypropylene hybrid fiber-reinforced concrete", Construction and Building Materials, 19(1), pp. 1–9, 2005. https://doi.org/10.1016/J.CONBUILDMAT.2004.05.002

[14] Ilg, P., Hoehne, C., Guenther, E. "High-performance materials in infrastructure: A review of applied life cycle costing and its drivers - The case of fiber-reinforced composites", Journal of Cleaner Production, 112, pp. 926–945, 2016. https://doi.org/10.1016/j.jclepro.2015.07.051

[15] Özbay, E., Karahan, O., Lachemi, M., Hossain, K. M. A., Atis, C. D. "Dual effectiveness of freezing-thawing and sulfate attack on high-volume slag-incorporated ECC", Composites Part B: Engineering, 45(1), pp. 1384–1390, 2013. https://doi.org/10.1016/j.compositesb.2012.07.038

[16] Kewalramani, M. A., Mohamed, O. A., Syed, Z. I. "Engineered Cementitious Composites for Modern Civil Engineering Structures in Hot Arid Coastal Climatic Conditions", Procedia Engineering, 180, pp. 767–774, 2017. https://doi.org/10.1016/j.proeng.2017.04.237

[17] Mohammed, B. S., Nuruddin, M. F., Aswin, M., Mahamood, N., Al-Mattarneh, H. "Structural Behavior of Reinforced Self-Compacted Engineered Cementitious Composite Beams", Advances in Materials Science and Engineering, 2016, 5615124, 2016. https://doi.org/10.1155/2016/5615124

[18] Li, M., Li, V. C. "Rheology, fiber dispersion, and robust properties of engineered cementitious composites", Materials and Structures, 46, pp. 405–420, 2013. https://doi.org/10.1617/s11527-012-9909-z

[19] Zhang, J., Leung, C. K. Y., Gao, Y. "Simulation of crack propagation of fiber reinforced cementitious composite under direct tension", Engineering Fracture Mechanics, 78(12), pp. 2439–2454, 2011. https://doi.org/10.1016/j.engfracmech.2011.06.003

[20] Maalej, M., Zhang, J., Quek, S. T., Lee, S. C. "High-velocity impact resistance of hybrid-fiber Engineered Cementitious Composites", In: Proceedings of the 5th International Conference on Fracture Mechanics of Concrete and Concrete Structures (FraMCos-5), Vail, CO, USA, 2004, pp. 1051–1058.

[21] Maalej, M., Leong, K. S. "Engineered cementitious composites for effective FRP-strengthening of RC beams", Composites Science and Technology, 65(7–8), pp. 1120–1128, 2005. https://doi.org/10.1016/j.compscitech.2004.11.007

[22] Maalej, M., Li, V. C. "Introduction of strain-hardening engineered cementitious composites in design of reinforced concrete flexural members for improved durability", ACI Structural Journal, 92(2), pp. 167–176, 1995. https://doi.org/10.14359/1150

[23] Maalej, M., Ahmed, S. F. U., Paramasivam, P. "Corrosion durability and structural response of functionally-graded concrete beams", Journal of Advanced Concrete Technology, 1(3), pp. 307–316, 2003. https://doi.org/10.3151/jact.1.307

[24] Hemmati, A., Kheyroddin, A., Sharbatdar, M. K. "Increasing the flexural capacity of RC beams using partially HPFRCC layers", Computers and Concrete, 16(4), pp. 545–568, 2015. https://doi.org/10.12989/cac.2015.16.4.545

[25] Yuan, F., Pan, J., Leung, C. K. Y. "Flexural Behaviors of ECC and Concrete/ECC Composite Beams Reinforced with Basalt Fiber-Reinforced Polymer", Journal of Composites for Construction, 17(5), pp. 591–602, 2013. https://doi.org/10.1061/(asce)cc.1943-5614.0000381

[26] Hou, L., Xu, S., Liu, H., Chen, D. "Flexural and interface behaviors of reinforced concrete/ultra-high toughness cementitious composite (RC/UHTCC) beams", Journal of Advanced Concrete Technology, 13(2), pp. 82–93, 2015. https://doi.org/10.3151/jact.13.82

[27] Zhang, J., Leung, C. K. Y., Cheung, Y. N. "Flexural performance of layered ECC-concrete composite beam", Composites Science and Technology, 66(11–12), pp. 1501–1512, 2006. https://doi.org/10.1016/j.compscitech.2005.11.024

[28] ASTM "ASTM C128 Standard Test Method for Density, Relative Density (Specific Gravity), and Absorption of Fine Aggregate", ASTM International, West Conshohocken, PA, USA, 2022.

[29] ASTM "ASTM C 29 Standard Test Method for Bulk Density ("Unit Weight") and Voids is Aggregate", ASTM International, West Conshohocken, PA, USA, 2017.

[30] ASTM "ASTM C136 Standard Test Method for Sieve Analysis of Fine and Coarse Aggregates", ASTM International, West Conshohocken, PA, USA, 2019.

[31] ASTM "ASTM C127 Standard Test Method for Relative Density (Specific Gravity) and Absorption of Coarse Aggregate", ASTM International, West Conshohocken, PA, USA, 2015.

[32] ASTM "ASTM C-1017 Standard Specification for Chemical Admixtures for Use in Producing Flowing Concrete", ASTM International, West Conshohocken, PA, USA, 2013.

[33] ASTM "ASTM A615 Standard Specification for Deformed and Plain Carbon-Steel Bars for Concrete Reinforcement", ASTM International, West Conshohocken, PA, USA, 2022. https://doi.org/10.1520/A0615_A0615M-22

[34] Lepech, M. D., Li, V. C. "Large-scale processing of engineered cementitious composites", ACI Materials Journal, 105(4), pp. 358–366, 2008.
https://doi.org/10.14359/19897

[35] ACI "301M-05 Specifications for Structural Concrete: General Requirements", American Concrete Institute, Farmington Hills, MI, USA, 2005.

[36] ASTM "C143/C143M-20 Standard Test Method for Slump of Hydraulic-Cement Concrete", ASTM International, West Conshohocken, PA, USA, 2020.
https://doi.org/10.1520/C0143_C0143M-20

[37] Kong, H.-J., Bike, S. G., Li, V. C. "Development of a self-consolidating engineered cementitious composite employing electrosteric dispersion/stabilization", Cement and Concrete Composites, 25, pp. 301–309, 2003.

[38] ASTM "ASTM C78/C78M-22 Standard Test Method for Flexural Strength of Concrete (Using Simple Beam with Third Point Loading)", ASTM International, West Conshohocken, PA, USA, 2022.
https://doi.org/10.1520/C0078_C0078M-22